Heterogeneous Catalysis

DOI: 10.1002/ange.201006155

Polyoxometalate Nanocone Nanoreactors: Magnetic Manipulation and Enhanced Catalytic Performance**

*Amjad Nisar, Yao Lu, Jing Zhuang, and Xun Wang**

Rationally designed assembly structures are of high scientific and technological importance for the development of multifunctional materials and devices.[1] Among various types of nanobuilding blocks, polyoxometalates (POMs) are a class of metal oxide nanoclusters that offer rich structural versatility and enormous applications.[2] The recent progresses in the synthesis of POM-based amphiphilic units have revolutionized POM chemistry, and consequently a variety of robust and well-defined assembly architectures with tunable properties have been developed, including one-dimensional wires[3] and fibers,[4] two-dimensional thin-films[5] and disks,[6] and three-dimensional vesicles,[7] spheres,[8] tubes,[6,9] and flowers.[10] Although, these assembly structures hold great promise for the design of new functional materials, in reality they have been less explored for their potential use in various scientific fields.

POMs have been extensively applied as catalysts for the oxidation of a variety of compounds such as alkenes, alcohols, and sulfides.[11] Particularly, the oxidation of sulfides to sulfones, which is environmentally highly important, yet brings up a key challenge.[12] To meet this challenge, many strategies in both homogeneous and heterogeneous catalytic reaction systems have been developed. The homogeneous approaches utilize the POM catalyst in bare form or in combination with a phase-transfer reagent, which generally have drawbacks associated with difficult catalyst separation and recovery.[13] The heterogeneous approaches involve encapsulation with specific cations, immobilization of POM into silica or polymer matrices, or microemulsion formation.[14] Although, heterogeneous systems provide easier catalyst recovery, generally it is based on filtration, which may be highly cumbersome on an industrial scale. In addition, the immobilization of POMs in supporting matrices involves complicated and lengthy catalyst preparation processes.[14f,15] Therefore, alternative multifunctional and superior approaches are needed. Recently, we reported well-defined, robust Keggin ion based nanocones, obtained by a simple and fast synthesis technique at room temperature.[6] Herein, we report the functionalization of nanocones with magnetite nanocrystals and their controlled manipulation in the reaction system. For example, we applied these nanocones for the catalytic oxidation of sulfides in which they act as nanoreactors to provide enhanced efficiency, selectivity, and easier recovery under an external magnetic field.

Figure 1 illustrates the concept of the nanocone nanoreactors. According to the accepted mechanism for the increased efficiency of the POM hybrid building block $(DODA)_3PW_{12}O_{40}$ (DODA = dimethyldioctadecylammonium) relative to that of bare $H_3PW_{12}O_{40}$, the highly hydrophobic alkyl chains attached on the $PW_{12}O_{40}^{3-}$ surface encapsulate the relatively nonpolar substrate (sulfide) molecules as a result of hydrophobic interactions, but easily release the product molecules (sulfone), which have much higher polarity.[14f] Thus, the alkyl chains act as a dynamic trap to enhance the probability of an interaction between the substrate and the catalytic center ($PW_{12}O_{40}^{3-}$). From this fact, we may hypothesize that the hybrid building blocks in the nanocone assemblies may provide more-enhanced catalytic efficiency due to self-organization of the building blocks in compact lamellar patterns (XRD; see Figures S4 and S5 in the Supporting Information) and thus increase in alkyl-chain

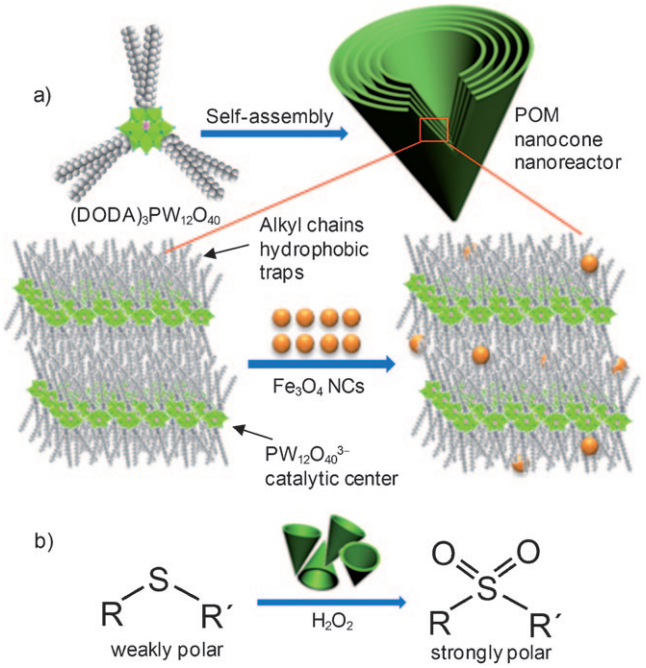

Figure 1. a) Schematic illustration of a POM nanocone nanoreactor. b) Oxidation of sulfides to sulfones in the presence of the cones as a catalyst.

[*] A. Nisar, Y. Lu, J. Zhuang, X. Wang
Department of Chemistry, Tsinghua University
Beijing 100084 (P.R. China)
E-mail: wangxun@mail.tsinghua.edu.cn

[**] This work was supported by NSFC (20971078, 20725102, 20921001), the Fok Ying Tung Education Foundation (111012), and the State Key Project of Fundamental Research for Nanoscience and Nanotechnology (2011CB932402).

Supporting information for this article is available on the WWW under http://dx.doi.org/10.1002/anie.201006155.

density around the catalytic center. While being functionalized with magnetite nanocrystals (NCs), the nanocones provide an advanced and swift method of catalyst recovery from the reaction system under an external magnetic field.

The supramolecular nanobuilding block $(DODA)_3PW_{12}O_{40}$ was prepared by ion exchange reaction between DODABr and phosphotungstic acid ($H_3PW_{12}O_{40}$),[6] and characterized by fundamental analytical techniques (see the Supporting Information). Figure 2a shows a scanning electron microscopy (SEM) image of nanocones obtained from the optimized mixed solvent system of chloroform and *n*-butanol (2:1.15, v/v) after about 20 min of ageing. It is evident that the cones are highly pure in morphology and can be obtain in bulk scale (Figure S8 in the Supporting Information). Further, static contact angle measurements revealed that the external surface of the cone assemblies comprises alkyl chains of the highly hydrophobic surfactant (Figure 2a, inset). It is important to note that the preparation of the cones is very fast (15–20 min at room temperature) and involves only a single-step synthesis. We think this promising fact is significant for their easier application in several fields.

Nanoscale incorporation of the ferromagnetic NCs into the assembly structures is an effective technique to develop functional nanomaterials with advanced applications in various areas.[16] We selected magnetite (Fe_3O_4) NCs (6–7 nm) for their excellent ferromagnetic properties (Figure 2f). Composite nanocones with incorporated magnetite NCs were obtained by a simple and fast synthesis approach (Figure 1). Figure 2b shows a low-resolution transmission electron microscope (TEM) image of the corresponding composite cones. The high-resolution TEM measurements of different regions of the cones clearly indicate the presence of magnetite NCs in the multilamellar cone assemblies (Figure 2c–e). Energy dispersive spectroscopy coupled with TEM further confirmed the existence of magnetite NCs and verified the TEM results (Figure S6 in the Supporting Information). The incorporation of magnetite NCs does not influence the self-organization of the nanobuilding blocks into a lamellar pattern nor the resultant assembly's conical shape. This fact may be attributed to the relatively small quantity of magnetite NCs relative to the number of POM building blocks. We observed that magnetite NCs exhibit strong affinity for the cone assemblies and rapidly adsorb on their surface when they were dispersed (in powder form) into the nanocone solution.

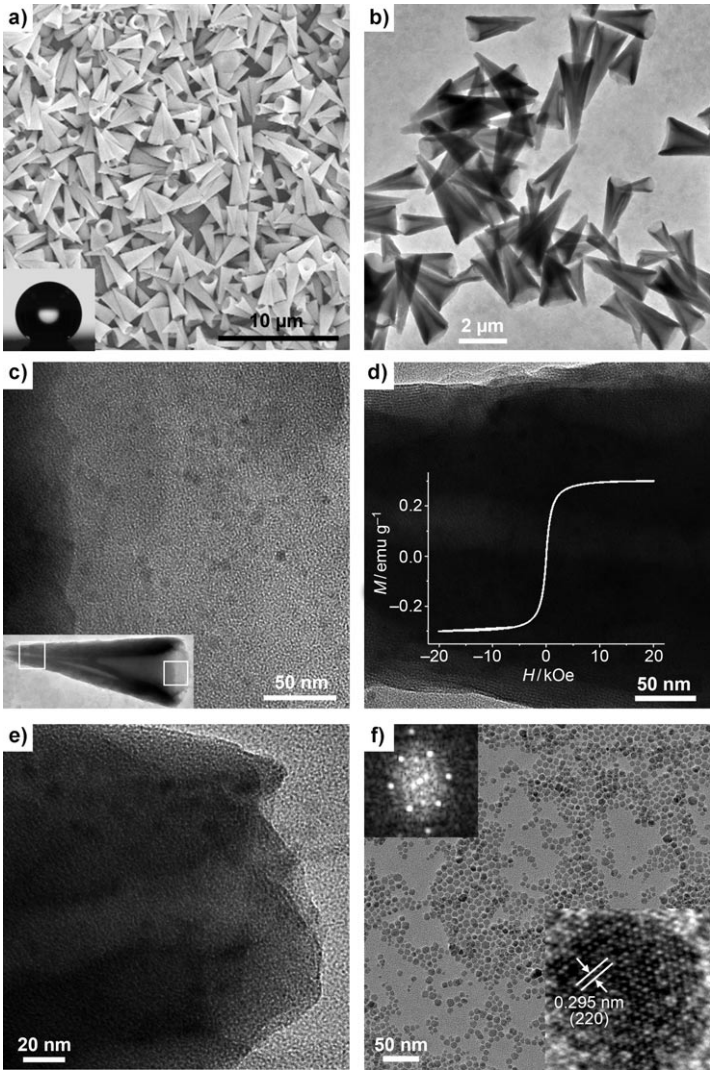

Figure 2. a) SEM image of $(DODA)_3PW_{12}O_{40}$ cones. Inset: static contact angle of a film of cones (146°). b) TEM image of the cones functionalized with magnetite NCs. c, d) Magnified TEM images of different areas of a cone, clearly indicating the magnetite NCs. The inset in (c) is the respective cone, highlighting the magnified areas. The inset in (d) is the magnetization curve of such cones. e) Tip of a cone at higher magnification. f) TEM image of magnetite NCs. The insets are a high-resolution TEM image of a magnetite NC and the corresponding fast Fourier transform (FFT) analysis.

The nanocones containing magnetite NCs were found to be sufficiently robust, stable, and physically manipulatable under an external magnetic field in petroleum fuel solvents such as *n*-hexane, cyclohexane, and *n*-dodecane. The real-time-controlled manipulation of the nanocones was examined by optical microscopy. A small magnet bar was used as external manipulator. Figure 3 shows a series of optical microscope images in the presence and absence of the manipulating force in *n*-hexane. In the absence of an external magnetic field the cone assemblies exhibit Brownian movement, whereas with the application of magnetic field all assemblies are transported quickly toward the magnet. The transportation direction and speed were found to be highly controllable and adjustable depending on the magnet position and strength. It is interesting to note that in the presence of a magnetic field the cones orient and transport in such a way that their open end leads the sharp tip (Figure 3b–d, f–i). We suppose this behavior may result from the relatively greater number of magnetite NCs at the larger open end. Moreover, continuous application of a magnetic field self-aligns the cones in rows (Figure 3d,i). Notably, however, the cones become separated and start Brownian motion with removal of the external magnetic field (Figure 3e), which we think eliminates any possibility of permanent self-aggregation and will be vital for their practical applications, for example, in catalysis.

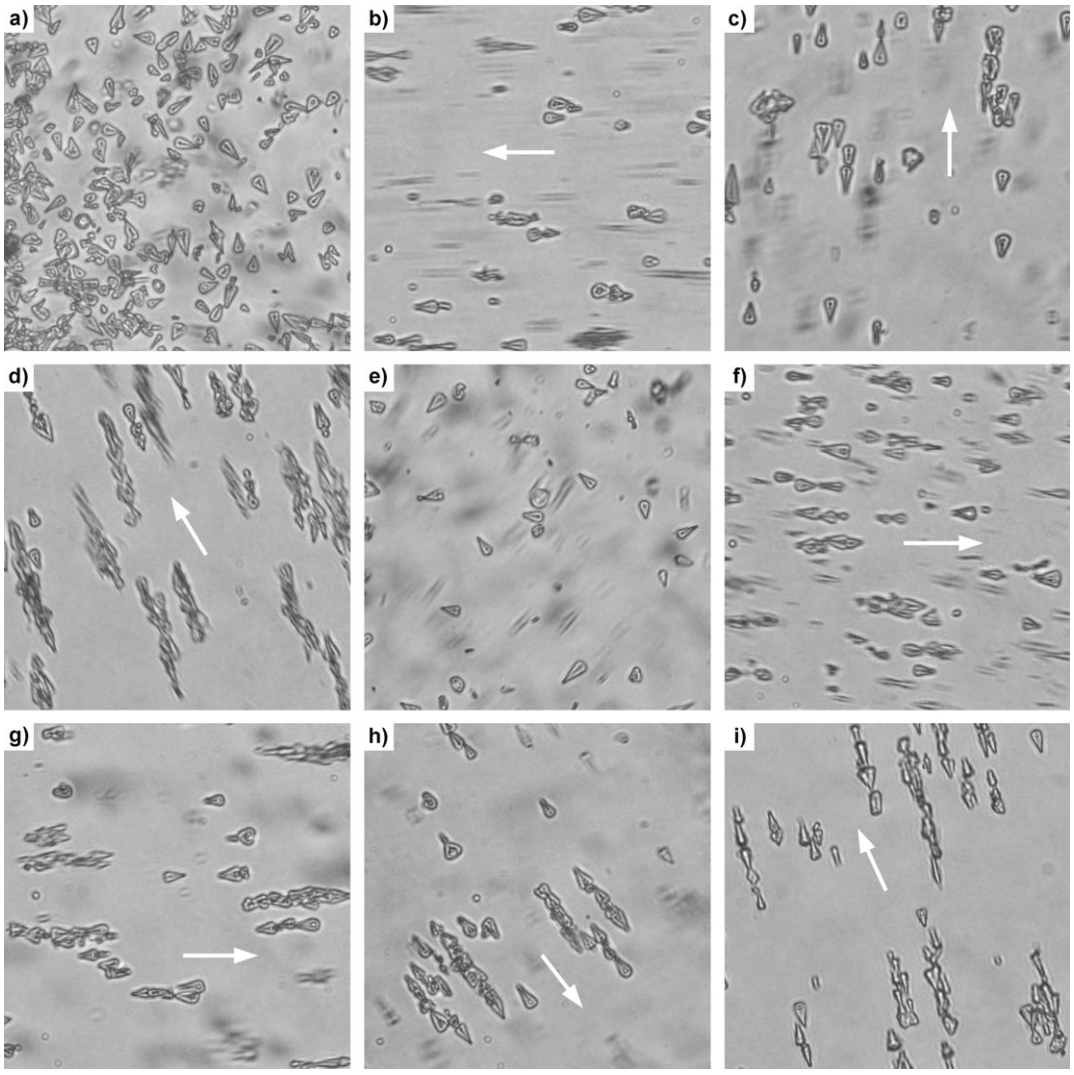

Figure 3. Optical microscopy study of the manipulation of $(DODA)_3PW_{12}O_{40}$ cones functionalized with magnetite NCs. The arrows indicate the direction of movement of the cones and the position of the manipulator (magnet). a) Cones in the state of Brownian motion. b,c) Nanocones controlled movement in the marked directions. d) Cones self-alignment in rows and movement in the direction of the applied magnetic field. e) Cones after removal of the magnetic field in state of Brownian motion. f–i) Manipulation of cones in various directions.

Sufficient magnetization ability of magnetic materials is an essential requirement for their remote and controlled manipulation in a reaction system. To further explore and estimate the magnetic properties of the nanocone assemblies carrying magnetite NCs, the magnetization curve at room temperature was plotted (inset in Figure 2d) revealing superparamagnetic behavior of the composite assemblies without the formation of a hysteresis loop, which we think is the key factor of self-alignment and redispersion of the cones in the presence and absence of an external magnetic field, respectively. The saturation magnetization of the composite cones ($0.29\ emu\,g^{-1}$) was found to be considerably below that of pure magnetite NCs ($15\ emu\,g^{-1}$) of similar size, which may be attributed to the fairly small amount of magnetite NCs incorporated in the cones.[17] However, the saturation magnetization value also provides a good estimate of the amount of magnetite NCs in the cones.

Owing to its facile, reversible electron-transfer ability, high thermal and chemical stability, and photochemical activity, Keggin ion $PW_{12}O_{40}^{3-}$ is a promising choice as a catalyst for oxidation reactions.[2j,11b,14f] To evaluate the catalytic properties of the nanocones, we selected sulfur-containing compounds such as dibenzothiophene (DBT), diphenyl sulfide (DPS), and dimethyl sulfide (DMS), for their selective conversion into sulfones. Hydrogen peroxide (30%) was selected as an oxidant, and *n*-hexane was chosen as solvent because of its low boiling point and thus ease of sample preparation for high performance liquid chromatography (HPLC) analysis.

Figure 4b demonstrates the progress of the DBT oxidation reaction with time. From the chromatograms, it is apparent that the DBT peak area (at $t_R = 5.15$ min) rapidly decreases with increase in reaction time and reaches almost to zero in about 38 min, whereas the peak area of dibenzothio-

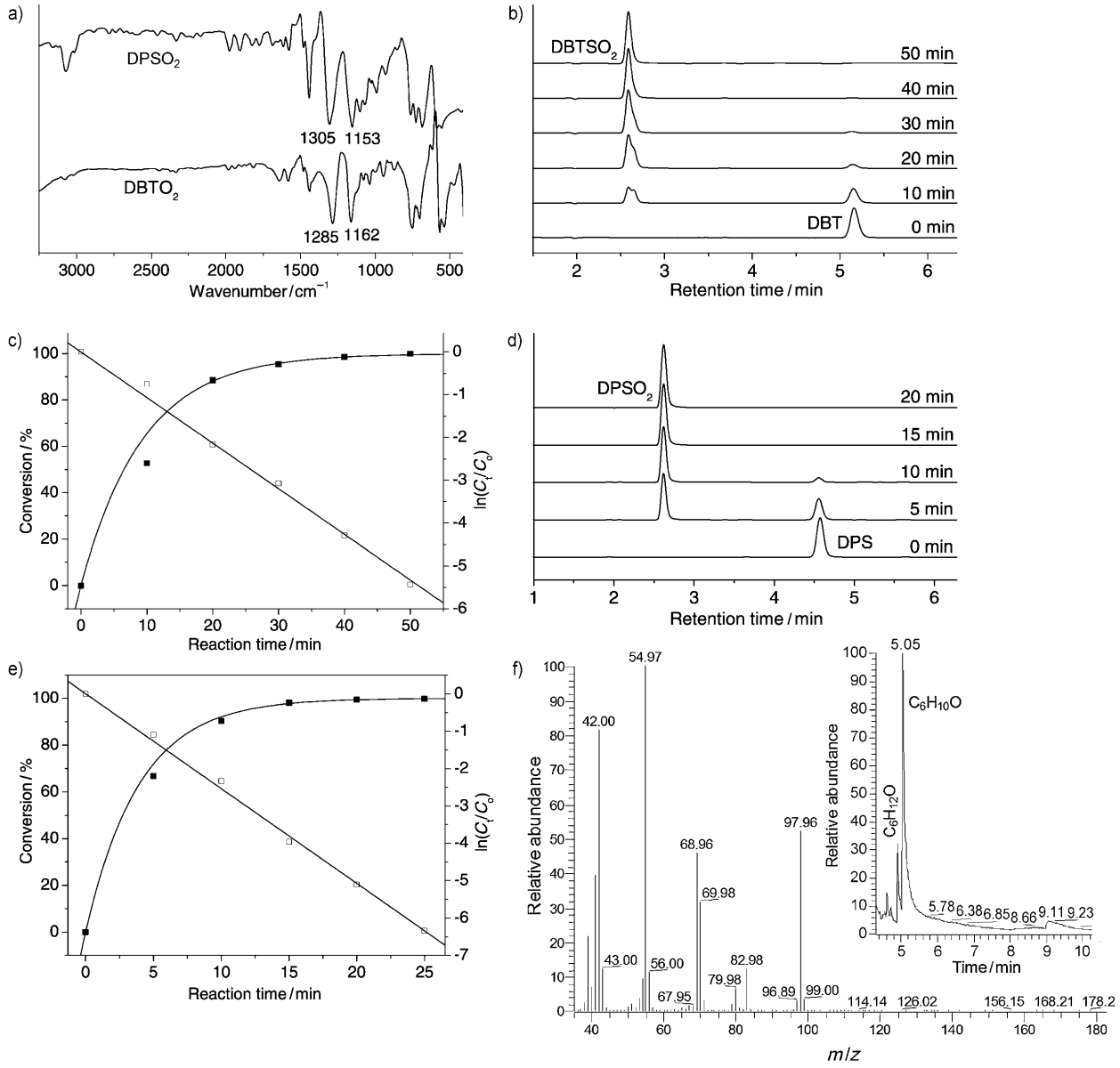

Figure 4. a) FTIR spectra of dibenzothiophene sulfone ($DBTO_2$) and diphenyl sulfone ($DPSO_2$). b) HPLC analysis of the oxidation of DBT catalyzed by $(DODA)_3PW_{12}O_{40}$ nanocones at various time intervals at 50 °C. c) DBT oxidation conversion and $\ln(C_t/C_0)$ versus the reaction time. d) HPLC analysis of the oxidation of DPS catalyzed by nanocones at various time intervals at 50 °C. e) DPS oxidation conversion and $\ln(C_t/C_0)$ versus the reaction time. f) MS spectra of the ketonization reaction product cyclohexanone. The inset shows the corresponding GC chromatogram, revealing the cyclohexanol and cyclohexanone signals.

phene sulfone ($t_R = 2.58$ min) rapidly increases and reaches a maximum value in about 38 min. The identification of the reaction product $DBTO_2$ was further confirmed by the presence of two strong bands (1285 cm^{-1} SO_2 asymmetric, 1162 cm^{-1} SO_2 symmetric) in the Fourier transform (FT) IR spectrum and by mass spectrometry (MS) measurements (Figure 4a and Figure S9 in the Supporting Information). To compare the catalytic efficiency of the nanocones with the that of the building block monomers, we also performed the DBT oxidation reaction by replacing the nanocones with the building block monomers. The catalytic efficiency of the monomers was found to be notably lower with reaction times of more than 2 h. The lower efficiency of the building block monomers may result from the lower density of hydrophobic alkyl chains around the POM catalytic centers relative to the cone assemblies.

Further, to understand the kinetics of the reaction, DBT conversion and $\ln(C_t/C_0)$ were plotted against reaction time (Figure 4c; C_0 and C_t symbolize the initial concentration and the concentration at time t of DBT). The linear fit to the experimental data demonstrates that the nanocone-based catalytic reaction agrees well with the reported homogeneous and heterogeneous catalytic reaction systems and follows pseudo-first-order reaction kinetics.[13a,14f] The corresponding equations are given in the Supporting Information. From the linear fit, the reaction rate constant k was calculated to be

$0.1066\ min^{-1}$, which indicates that the nanocones exhibit high efficiency for the oxidation of DBT. Moreover, as the *k* value lies between those for bare POM (homogeneous)[13a] and immobilized POM (heterogeneous)[14f] oxidative catalytic reaction systems, we suspect that the nanocones form a quasi-homogeneous catalytic reaction system. The oxidation of DPS to diphenyl sulfone also obeys the pseudo-first-order reaction kinetics (Figure 4d,e), and the reaction is complete with 100% selectivity in about 20 min, which further reveals the high efficiency of the nanocone assemblies. The nanocone assemblies were not only found to be efficient and highly selective catalysts for the conversion of DBT and DPS but also for that of DMS. The reaction time for 100% conversion was estimated to be about 20 min by MS measurements (Figure S11 in the Supporting Information).

In an extension of our work, we also tested the nanocones for other types of oxidation reactions: the catalytic ketonization of alcohols and the epoxidation of alkenes. The catalytic reactions were performed in *n*-hexane for 8 h with a similar molar ratio between substrate and catalyst as was used for the sulfides. The cones catalyzed the oxidation of cyclohexanol to cyclohexanone with about 90% conversion and high selectivity (100%) (Figure 4f) and the epoxidation of 1-octadecene to 1,2-epoxyoctane with the same high selectivity but with a conversion of only 30% (Figure S12 in the Supporting Information). The low efficiency for the epoxidation reaction may be attributed to an inappropriate solvent system, oxidizing reagent, or other experimental conditions. In future work, we aim to investigate and optimize the reaction conditions to enhance the catalytic efficiency of the nanocones for epoxidation reactions.

The bare Keggin anion $PW_{12}O_{40}^{3-}$ readily reacts with H_2O_2 and degrades to Venturello complexes and peroxometalate species.[18] Thus, to investigate the stability of the POM building block $(DODA)_3PW_{12}O_{40}$ and the cone assemblies, we characterized the catalyst after the oxidation reaction. The elemental analysis, optical microscopy, FTIR, solid-state ^{31}P NMR, and ^{31}P NMR ($CDCl_3$ solution) spectroscopy demonstrate that the assembly structure is highly stable and retains the Keggin ion identity and conical shape (Figures S13–S16 in the Supporting Information). Further, the recent reports about surfactant-encapsulated POM-based recoverable and reusable oxidation catalysts support our results.[14a,c,f] Although the catalytic reaction mechanism is ambiguous, we speculate that, firstly, oxidant H_2O_2 reacts with the POM to form the active polyperoxometalate, which subsequently oxidizes the substrate molecule and returns to the original Keggin ion state.

In conclusion, we have functionalized POM nanocone assemblies by the incorporation of magnetite nanocrystals for their advanced and controlled manipulation in various reaction systems. The nanospaces and increased surfactant alkyl chain density around the POM in the nanocones provide enhanced catalytic performance for the oxidation of sulfides to sulfones. Thus, the nanocones perform as promising nanoreactors to provide enhanced catalytic activity and advanced recovery by an external magnetic field. In addition, the nanocones can be applied for other oxidation reactions such as ketonization and epoxidation. Their hollow interior allows these cones to act as nanovehicles to transport foreign materials to target spaces.

Received: October 1, 2010
Revised: January 28, 2011
Published online: March 2, 2011

Keywords: heterogeneous catalysis · magnetic properties · nanostructures · polyoxometalates

[1] a) X. Wang, J. Zhuang, Q. Peng, Y. Li, *Nature* **2005**, *437*, 121–124; b) J.-F. Lemonnier, S. Floquet, J. Marrot, E. Cadot, *Eur. J. Inorg. Chem.* **2009**, 5233–5239; c) R. J. Brea, C. Reiriz, J. R. Granja, *Chem. Soc. Rev.* **2010**, *39*, 1448–1456; d) R. Tenne, M. Redlich, *Chem. Soc. Rev.* **2010**, *39*, 1423–1434; e) P.-P. Wang, B. Bai, S. Hu, J. Zhuang, X. Wang, *J. Am. Chem. Soc.* **2009**, *131*, 16953–16960; f) D.-L. Long, E. Burkholder, L. Cronin, *Chem. Soc. Rev.* **2007**, *36*, 105–121; g) Y. Wang, H. Xu, X. Zhang, *Adv. Mater.* **2009**, *21*, 2849–2864; h) X. Xu, X. Wang, A. Nisar, X. Liang, J. Zhuang, S. Hu, Y. Zhuang, *Adv. Mater.* **2008**, *20*, 3702–3708.

[2] a) M. T. Pope, A. Müller, *Angew. Chem.* **1991**, *103*, 56–70; *Angew. Chem. Int. Ed. Engl.* **1991**, *30*, 34–48; b) P. Gouzerh, A. Proust, *Chem. Rev.* **1998**, *98*, 77–112; c) A. Müller, F. Peters, M. T. Pope, D. Gatteschi, *Chem. Rev.* **1998**, *98*, 239–272; d) S. S. Mal, U. Kortz, *Angew. Chem.* **2005**, *117*, 3843–3846; *Angew. Chem. Int. Ed.* **2005**, *44*, 3777–3780; e) T. Mitra, P. Miró, A.-R. Tomsa, A. Merca, H. Bögge, J. B. Ávalos, J. M. Poblet, C. Bo, A. Müller, *Chem. Eur. J.* **2009**, *15*, 1844–1852; f) A. Müller, F. L. Sousa, A. Merca, H. Bögge, P. Miró, J. A. Fernández, J. M. Poblet, C. Bo, *Angew. Chem.* **2009**, *121*, 6048–6051; g) J. Zhang, J. Hao, Y. Wei, F. Xiao, P. Yin, L. Wang, *J. Am. Chem. Soc.* **2010**, *132*, 14–15; h) H. N. Miras, G. J. T. Cooper, D.-L. Long, H. Bögge, A. Müller, C. Streb, L. Cronin, *Science* **2010**, *327*, 72–74; i) X. Fang, M. Speldrich, H. Schilder, R. Cao, K. P. O'Halloran, C. L. Hill, P. Kogerler, *Chem. Commun.* **2010**, *46*, 2760–2762; j) M. Sadakane, E. Steckhan, *Chem. Rev.* **1998**, *98*, 219–238.

[3] Z. Kang, E. Wang, M. Jiang, S. Lian, *Nanotechnology* **2004**, *15*, 55–58.

[4] M. Carraro, A. Sartorel, G. Scorrano, C. Maccato, M. H. Dickman, U. Kortz, M. Bonchio, *Angew. Chem.* **2008**, *120*, 7385–7389; *Angew. Chem. Int. Ed.* **2008**, *47*, 7275–7279.

[5] a) Y.-Y. Bao, L.-H. Bi, L.-X. Wu, S. S. Mal, U. Kortz, *Langmuir* **2009**, *25*, 13000–13006; b) M. Clemente-León, E. Coronado, C. J. Gómez-García, C. Mingotaud, S. Ravaine, G. Romualdo-Torres, P. Delhaès, *Chem. Eur. J.* **2005**, *11*, 3979–3987; c) S. Liu, D. G. Kurth, B. Bredenkötter, D. Volkmer, *J. Am. Chem. Soc.* **2002**, *124*, 12279–12287.

[6] A. Nisar, J. Zhuang, X. Wang, *Chem. Mater.* **2009**, *21*, 3745–3751.

[7] a) J. Zhang, Y.-F. Song, L. Cronin, T. Liu, *J. Am. Chem. Soc.* **2008**, *130*, 14408–14409; b) Y. Yan, B. Li, W. Li, H. Li, L. Wu, *Soft Matter* **2009**, *5*, 4047–4053; c) W. Bu, S. Uchida, N. Mizuno, *Angew. Chem.* **2009**, *121*, 8431–8434; *Angew. Chem. Int. Ed.* **2009**, *48*, 8281–8284.

[8] a) H. Li, H. Sun, W. Qi, M. Xu, L. Wu, *Angew. Chem.* **2007**, *119*, 1322–1325; *Angew. Chem. Int. Ed.* **2007**, *46*, 1300–1303; b) A. Nisar, X. Xu, S. Shen, S. Hu, X. Wang, *Adv. Funct. Mater.* **2009**, *19*, 860–865.

[9] C. Ritchie, G. J. T. Cooper, Y.-F. Song, C. Streb, H. Yin, A. D. C. Parenty, D. A. MacLaren, L. Cronin, *Nat. Chem.* **2009**, *1*, 47–52.

[10] A. Nisar, Y. Lu, X. Wang, *Chem. Mater.* **2010**, *22*, 3511–3518.

[11] a) N. Mizuno, K. Yamaguchi, K. Kamata, *Coord. Chem. Rev.* **2005**, *249*, 1944–1956; b) I. V. Kozhevnikov, *Chem. Rev.* **1998**, *98*, 171–198; c) M. V. Vasylyev, R. Neumann, *J. Am. Chem. Soc.*

2004, *126*, 884 – 890; d) W. Zhu, H. Li, X. Jiang, Y. Yan, J. Lu, L. He, J. Xia, *Green Chem.* **2008**, *10*, 641 – 646; e) R. Belanger, J. B. Moffat, *Environ. Sci. Technol.* **1995**, *29*, 1681 – 1685; f) K. Nomiya, Y. Sugaya, S. Sasa, M. Miwa, *Bull. Chem. Soc. Jpn.* **1980**, *53*, 2089 – 2090.

[12] a) I. Fernández, N. Khiar, *Chem. Rev.* **2003**, *103*, 3651 – 3706; b) P. De Filippis, M. Scarsella, *Energy Fuels* **2003**, *17*, 1452 – 1455.

[13] a) M. Te, C. Fairbridge, Z. Ring, *Appl. Catal. A* **2001**, *219*, 267 – 280; b) D. Huang, Y. J. Wang, L. M. Yang, G. S. Luo, *Ind. Eng. Chem. Res.* **2006**, *45*, 1880 – 1885.

[14] a) L. Plault, A. Hauseler, S. Nlate, D. Astruc, J. Ruiz, S. Gatard, R. Neumann, *Angew. Chem.* **2004**, *116*, 2984 – 2988; *Angew. Chem. Int. Ed.* **2004**, *43*, 2924 – 2928; b) A. Haimov, R. Neumann, *J. Am. Chem. Soc.* **2006**, *128*, 15697 – 15700; c) C. Li, Z. Jiang, J. Gao, Y. Yang, S. Wang, F. Tian, F. Sun, X. Sun, P. Ying, C. Han, *Chem. Eur. J.* **2004**, *10*, 2277 – 2280; d) C. Li, J. Gao, Z. Jiang, S. Wang, H. Lu, Y. Yang, F. Jing, *Top. Catal.* **2005**, *35*, 169 – 175; e) H. Lü, J. Gao, Z. Jiang, Y. Yang, B. Song, C. Li, *Chem. Commun.* **2007**, 150 – 152; f) W. Qi, Y. Wang, W. Li, L. Wu, *Chem. Eur. J.* **2010**, *16*, 1068 – 1078.

[15] K. Inumaru, T. Ishihara, Y. Kamiya, T. Okuhara, S. Yamanaka, *Angew. Chem.* **2007**, *119*, 7769 – 7772; *Angew. Chem. Int. Ed.* **2007**, *46*, 7625 – 7628.

[16] a) N. K. Shrestha, J. M. Macak, F. Schmidt-Stein, R. Hahn, C. T. Mierke, B. Fabry, P. Schmuki, *Angew. Chem.* **2009**, *121*, 987 – 990; *Angew. Chem. Int. Ed.* **2009**, *48*, 969 – 972; b) S.-H. Kim, J. Y. Sim, J.-M. Lim, S.-M. Yang, *Angew. Chem.* **2010**, *122*, 3874 – 3878; *Angew. Chem. Int. Ed.* **2010**, *49*, 3786 – 3790; c) S. Shylesh, V. Schünemann, W. R. Thiel, *Angew. Chem.* **2010**, *122*, 3504 – 3537; *Angew. Chem. Int. Ed.* **2010**, *49*, 3428 – 3459.

[17] X. Liang, X. Wang, J. Zhuang, Y. Chen, D. Wang, Y. Li, *Adv. Funct. Mater.* **2006**, *16*, 1805 – 1813.

[18] a) L. Salles, C. Aubry, R. Thouvenot, F. Robert, C. Doremieux-Morin, G. Chottard, H. Ledon, Y. Jeannin, J. M. Bregeault, *Inorg. Chem.* **1994**, *33*, 871 – 878; b) C. Aubry, G. Chottard, N. Platzer, J. M. Bregeault, R. Thouvenot, F. Chauveau, C. Huet, H. Ledon, *Inorg. Chem.* **1991**, *30*, 4409 – 4415.

